



Deposited via The University of Sheffield.

White Rose Research Online URL for this paper:

<https://eprints.whiterose.ac.uk/id/eprint/93423/>

Version: Accepted Version

---

**Article:**

Ascani, D., Mazza, C., De Lollis, A. et al. (2015) A procedure to estimate the origins and the insertions of the knee ligaments from computed tomography images. *Journal of Biomechanics*, 48 (2). pp. 233-237. ISSN: 0021-9290

<https://doi.org/10.1016/j.biomech.2014.11.041>

---

Article available under the terms of the CC-BY-NC-ND licence  
(<https://creativecommons.org/licenses/by-nc-nd/4.0/>)

**Reuse**

Items deposited in White Rose Research Online are protected by copyright, with all rights reserved unless indicated otherwise. They may be downloaded and/or printed for private study, or other acts as permitted by national copyright laws. The publisher or other rights holders may allow further reproduction and re-use of the full text version. This is indicated by the licence information on the White Rose Research Online record for the item.

**Takedown**

If you consider content in White Rose Research Online to be in breach of UK law, please notify us by emailing [eprints@whiterose.ac.uk](mailto:eprints@whiterose.ac.uk) including the URL of the record and the reason for the withdrawal request.

1 **A procedure to estimate the origins and the insertions of the knee**  
2 **ligaments from computed tomography images**

3 Daniele Ascani<sup>1,2\*</sup>, Claudia Mazzà<sup>1,2</sup>, Angelo De Lollis<sup>3</sup>, Massimiliano Bernardoni<sup>3</sup>, and  
4 Marco Viceconti<sup>1,2</sup>

5  
6 <sup>1</sup> Department of Mechanical Engineering, University of Sheffield, Sheffield UK

7 <sup>2</sup> INSIGNEO Institute for *in silico* Medicine, University of Sheffield, Sheffield UK

8 <sup>3</sup> Medacta International SA, Castel San Pietro, Switzerland

9  
10  
11  
12  
13  
14  
15  
16  
17  
18  
19 Submitted as Original Article to Journal of Biomechanics

20  
21  
22 \*Corresponding Author: Daniele Ascani

23  
24 Department of Mechanical Engineering  
25 INSIGNEO Institute for *in silico* Medicine  
26 Room C+13 - C+ Floor  
27 The Pam Liversidge Building, Sir Frederick Mappin Building  
28 Mappin Street, Sheffield S13JD  
29 United Kingdom  
30 Telephone#: +44 (0) 114 222 6174  
31 Fax#: +44 (0) 114 222 7890  
32 Email: dascani1@sheffield.ac.uk  
33

34 **Word count**

35 Abstract: 250 words

36 Introduction-Discussion: 3471 words

37 Tables: 6

38 Figures: 2

39  
40 **Keywords:**

41 Knee Ligaments, Affine Registration, Osteometric scaling, Procrustes Analysis

42 **ABSTRACT**

43 The estimation of the origin and insertion of the four knee ligaments is crucial for  
44 individualised dynamic modelling of the knee. Commonly this information is obtained *ex*  
45 *vivo* or from high resolution MRI, which are not always available. Aim of this work is to  
46 devise a method to estimate the origins and insertions from CT images. A reference  
47 registration atlas was created using a set of 16 bone landmarks visible in CT and 8 origins  
48 and insertions estimated from MRI and *in vitro* data available in the literature for three knees.  
49 This atlas can be registered to the set of bone landmarks palpated on any given CT using an  
50 affine transformation. The resulting orientation and translation matrices and scaling factors  
51 can be used to find also the ligament origin and insertions. This procedure was validated on  
52 seven pathological knees for which both CT and MRI of the knee region were available,  
53 using a proprietary software tool (NMSBuilder, SCS srl, Italy). To assess the procedure  
54 reproducibility and repeatability, four different operators performed the landmarks palpation  
55 on all seven patients. The average difference between the values predicted by registration on  
56 the CT scan and those estimated on the MRI was  $2.1 \pm 1.2$  mm for the femur and  $2.7 \pm 1.0$  mm  
57 for the tibia, respectively. The procedure is highly repeatable, with no significant differences  
58 observed within or between the operators ( $p > 0.1$ ) and allows to estimate origins and  
59 insertions of the knee ligaments from a CT scan with the same level of accuracy obtainable  
60 with MRI.

61

62

63

64

## 65 INTRODUCTION

66 The main role of the ligaments, which connect bone with bone, is to provide mechanical  
67 stability to the joints, guiding their movements and preventing excessive motion. The knee is  
68 the largest and complex joint of the human body and has four major ligaments: Medial  
69 Collateral (MCL), Lateral Collateral (LCL), Anterior Cruciate (ACL) and Posterior Cruciate  
70 (PCL). In clinical applications and biomedical research individualised musculoskeletal  
71 models are currently used for many purposes such customized prosthetic implants (Bert,  
72 1996; Reggiani et al., 2007), computer-aided surgery (Zanetti et al., 2005), gait analysis  
73 (Kepple et al., 1997) or automated image segmentation (Ellingsen et al., 2010). In  
74 orthopaedic surgery a geometric model of the patient's bone can reproduce the basic  
75 morphometry in order to perform a correct computer based surgery (Radermacher et al.,  
76 1998). In gait analysis an accurate geometrical model is fundamental to create a realistic  
77 musculoskeletal model (Kepple et al., 1997).

78 Many computational dynamic models of the knee have been developed (Arnold et al., 2010;  
79 Blankevoort and Huiskes, 1996; Guess et al., 2011; Kia et al., 2014; Shelburne and Pandy,  
80 2002) to understand the forces and the strains on the knee structures, such as the ligaments,  
81 during static and locomotion activities. Improving the accuracy of these models could help to  
82 discover the causes of ligaments' injury and guide the surgical treatment in order to improve  
83 the functional outcome (Woo et al., 2006). A subject specific model of the knee is also  
84 essential for total knee arthroplasty in the preoperative phase in order to assure the durability  
85 and the reliability of the joint implant especially for younger patient with a greater physical  
86 activity (Zanetti et al., 2005). The accurate estimation of the origin and insertion of these  
87 ligaments is a crucial step in all the above applications.

88 Subject specific models of the knee can be generated using information obtained either *ex*  
89 *vivo*, probing fresh cadavers, or from high resolution Magnetic Resonance Imaging (MRI).

90 Brand et al. (1982) used measurement on three cadavers to obtain a set of lower extremity  
91 origin and insertion coordinates. These procedures are complex and cumbersome, therefore  
92 many studies utilized a few number of specimens, limiting the impact of the findings. In  
93 addition, the data obtained from cadavers have proven to be valid for modelling the knees  
94 they have been acquired for, but may likely not translate to other subjects (H. Bloemker,  
95 2012). Many studies proposed methods to create subject specific model by scaling a generic  
96 template in order to measure inaccessible point such as the origin and insertions of the knee  
97 ligaments (Brand et al., 1982; Lewis et al., 1980). This procedure that involves the scaling of  
98 a generic template provides to build one cloud of palpable points on a cadaver specimen and  
99 corresponding points on the *in vivo* subject. Calculating the transformation between these  
100 two landmark clouds allows measuring inaccessible points.

101 The parameters needed to determine a rigid body transformation are a rotation matrix, a  
102 translation vector and a scaling factor. Lew and Lewis (1977) demonstrated that the  
103 application of data obtained from cadavers directly to *in vivo* subject is not suitable, some  
104 kind of scaling is proper because of the dimension differences between the *in vivo* subject  
105 and the cadaveric specimens. Morrison (Morrison, 1970), in order to study the mechanics of  
106 knee joint in relation to normal walking, developed a technique to scale uniformly along the  
107 axes bony landmarks from dry bone data and an experimental subject. Lew and Lewis (1977)  
108 formulated a scaling technique that includes the Morrison method to scale inaccessible points  
109 from a dried bone specimen to an *in vivo* subject. This technique provides anisotropic scaling  
110 along three mutually orthogonal axes defined in both rigid bodies and is based on the use of  
111 four landmarks palpable on the subject and four on the corresponding specimen. The  
112 landmarks used to determine the rigid body transformation will contain some errors that  
113 come from the palpation of those points on the reference specimen and the experimental  
114 subject. Challis (1995) suggested a procedure using a linear least-square method which

115 attempted to take into account those errors. Unfortunately this method allows the calculation  
116 of the rigid body transformation parameters assuming that the scaling is uniform along the  
117 three axes. Anisotropic scaling technique has been presented by Lewis et al. (1980), using  
118 eight landmarks on both the specimen and the experimental subject, the results revealed that  
119 the anisotropic scaling was more accurate than the isotropic scaling.

120 In view of all that has been mentioned so far, it can be said that previous studies validated  
121 procedures that allow calculating inaccessible points on *in vivo* subjects using different  
122 osteometric scaling techniques. In these studies the analysis of human subject *in vivo* has  
123 been performed without using CT or MRI scan images. Since only a minimal set of skeletal  
124 landmarks can be palpated through external palpation, the number of the landmarks used in  
125 the previous methods was very low. Lewis et al. (1980) demonstrated that anisotropic scaling  
126 improves the identification of anatomical landmarks locations, particularly when a large  
127 number of points were used in the scaling. Also, a detailed description of the landmarks  
128 selected were not present in the previous studies, the lack of standard and well defined  
129 guidelines for the palpation of the these landmarks affects the accuracy of the rigid body  
130 registration (Van Sint Jan and Della Croce, 2005).

131 The purpose of this study was to create a procedure to estimate the origins and the insertions  
132 of the knee ligaments by: providing a reproducible and repeatable anatomical landmark cloud  
133 for virtual palpation, creating a registration atlas and using an affine transformation (rotation,  
134 translation, anisotropic scaling). The accuracy of this procedure will be assessed through  
135 comparison with results obtained from MRI.

136

137 **MATERIALS AND METHODS**

138 The dataset used in this study (D1) has been provided by Medacta International SA (Castel S.  
139 Pietro, Switzerland). It consists of seven set of images obtained from seven different patients  
140 ( $64 \pm 5$  years) who have undergone a Total Knee Replacement. Each patient's dataset  
141 includes Computed Tomography (CT) and Magnetic Resonance Imaging (MRI) of  
142 pathological knee that underwent surgery and the bone geometries obtained by segmenting  
143 the CT data. In addition to D1, a second dataset (D2) has been obtained from the multibody  
144 models of the human knee project (Guess et al., 2011, 2010; H. Bloemker, 2012). These  
145 models are based on three cadaver knees (Table 1) that have been mechanically tested in a  
146 dynamic knee simulator. Knee geometries (bone, cartilage, and menisci) were derived from  
147 MRI and ligament insertions were obtained from both MRI and probing the cadaver knees.  
148 D2 also contains information on ligament modelling, including the origin and insertion  
149 locations.

150 (Figure 1)

151 The first part of this study aims at creating a reproducible and repeatable bone landmarks  
152 cloud to be palpated on CT scan images. A detailed standard description of body landmarks  
153 through manual or virtual palpation is available in literature (van Sint Jan, 2007). Among  
154 these, a subset of landmarks (see Figure 2) belonging to the knee, tibia and fibula has been  
155 chosen. This landmark cloud has then been identified on each subject dataset through virtual  
156 palpation. NMSBuilder (SCS srl, Italy) has been used to visualize the 3D geometry and to  
157 perform the virtual palpation (location of anatomical points over a 3D visualisation) and the  
158 registration between the landmark clouds. The virtual palpation has been performed by four  
159 expert operators on both D1 and D2. Each operator performed the virtual palpation on ten  
160 knees (cases), repeating the operation three times for each knee (trials). Three operators  
161 performed the procedure using NMSBuilder, whereas the fourth one used an in-house tool

162 developed by Medacta International SA. Reproducibility and repeatability were assessed  
163 using repeated measures analysis of variance (ANOVA). In particular, a repeated measure  
164 ANOVA was performed for each operator considering the “case” as between group factor  
165 and the “trial” (3 levels) as within factor. Three separate ANOVA, one for each test, were  
166 then performed considering the operator as between group factor and the cases as within  
167 group factor (10 levels).

168 Once reproducibility and repeatability of the bone landmarks had been assessed, they were  
169 palpated on D2 in order to create a reference landmark cloud ( $C_R$ ), and on D1 in order to  
170 create a subject-specific landmark cloud ( $C_S$ ). Once palpated, the two clouds had to be  
171 registered. An affine transformation was used to this purpose. The method that allows the  
172 calculation of the parameters that describe an affine transformation between two paired  
173 landmark clouds is called, in statistical shape analysis, *Procrustes Analysis* (Grimpampi et al.,  
174 2014). In particular, the affine transformation that maps  $C_R$  to  $C_S$  is composed by a 3x3  
175 transformation matrix, which includes Translation ( $T = \langle T_x, T_y, T_z \rangle$ ), Rotation  
176 ( $R = \langle R_x, R_y, R_z \rangle$ ), and scaling ( $S = \langle S_x, S_y, S_z \rangle$ ) parameters. This operation is implemented in  
177 Lhp Builder following the method proposed by Berthold and Horn (1987). Once T, R and S  
178 are calculated, it is possible to register on  $C_S$  also those landmarks belonging only to  $C_R$ ,  
179 which, in our case, are the origins and insertions of the four knee ligaments. The ensemble of  
180  $C_R$  and of the eight origins and insertions of the knee ligaments composes the so-called  
181 Registration Atlas ( $RA$ ). The error associated to the registration procedure is called Procrustes  
182 Distances ( $PD$ ) and represents the geometric distance between  $C_S$  and  $C_R$ . These values  
183 estimate the accuracy of the procedure.

184 The scaling operation, necessary to take into account anthropometric differences due to age  
185 or gender (Fehring et al., 2009), might have as a consequence the fact that landmarks in  $C_R$   
186 are not always located on the bone surface. For this reason, a visual inspection needs to be

187 performed after the registration and adjustments need to be taken. These adjustments were  
188 performed using an ad-hoc Lhp Builder function, names “snap to surface”, which allows to  
189 move the landmark along the axes characterized by the minimal distance from the closest  
190 surface. The repeatability of this operation has been assessed by having one operator  
191 repeating it for three times on each case in D1 (after having performed the calculation of the  
192 origins and insertions of the knee ligaments using the RA, as described in the following  
193 paragraph).

194 Using the three models from the D2 dataset, four atlases were created: one for each model  
195 and one as the average of the previous three (Atlas 1, Atlas 2, Atlas 3, and Atlas M). Not  
196 having a proper gold standard available, the four atlases have been compared in terms of  
197 Procrustes Distance between the landmarks of  $C_R$  registered on the subjects and the  
198 landmarks of  $C_S$  palpated on the seven subjects.

199 Once the best RA had been selected, it was used to estimate the origin and the insertions of  
200 the knee ligaments of all the cases in D1. Initially, the origin and insertions were calculated  
201 through the affine transformation using the CT scan, successively the verification of the  
202 positions of those landmarks has been performed using MRI scan where it was possible to  
203 estimate the ligaments attachments. In NMSBuilder, the landmarks that represented the  
204 origins and insertions of the ligaments were moved whenever the position was considered  
205 wrong in according with those images. Then, we compared the distances between the data  
206 obtained from the CT scan with those corrected with MRI.

207

208

209

210

## 211 RESULTS

212 The results of the ANOVA performed on the data obtained from the various operators  
213 showed that the procedure is highly repeatable, with no significant differences observed  
214 within ( $p=0.748$  for trial 1,  $p=0.966$  for trail 2, and  $p=0.992$ , for trial 3, respectively) or  
215 between operators ( $p=0.430$  for operator 1,  $p=0.572$  for operator 2,  $p=0.187$  for operator 3,  
216 and  $p=0.685$  for operator 4, respectively). These findings suggest that changing the operator  
217 does not affect the repeatability and the reproducibility of the virtual palpation of the selected  
218 anatomical landmarks cloud. In contrast, the ANOVA revealed that the case factor influences  
219 the repeatability of the virtual palpation ( $p<0.001$ ): the specific morphology of a knee or the  
220 low resolution of the CT images can be a cause for lower precision in the identification of the  
221 landmarks.

222 Since there was no between-operators effect, the precision of the virtual palpation was  
223 evaluated in terms of standard deviation of the landmarks positions, palpated by the four  
224 operators over the three trials. The standard deviation ranged from 0.02 mm to 7.71 mm  
225 (Table 2).

226 The registration of the four Atlases (Atlas 1, Atlas 2, Atlas 3, Atlas M) on D2 revealed that  
227 the Atlas M gives the best result in terms of PD. The mean PD between the landmarks of  $C_R$   
228 registered on the seven subjects, and the landmarks of  $C_S$  palpated on the seven subjects (see  
229 Tables 3 and 4) was  $2.34 \pm 0.59$  mm for the femur and  $1.53 \pm 0.50$  mm for the tibia,  
230 respectively (averaged on the seven subjects).

231 The mean PD between the origin and insertions of ligaments calculated with the Registration  
232 Atlas M and those ones estimated from the MRI were  $2,3 \pm 0,3$  mm ( $0,4$  mm  $< PD < 3,9$  mm)  
233 on the femur and  $2,7 \pm 1,0$  mm ( $1,4$  mm  $< PD < 4,4$  mm) on the tibia (averaged over the seven  
234 subjects) (see Tables 5 and 6).

235 The “snap to surface” operation was highly repeatable, with the standard deviation of the  
236 position of the ligament attachments after the “snap to surface” ranging from 0 to 0.3 mm.

## 237 **DISCUSSION**

238 This study presented a procedure to estimate, with high accuracy, origins and insertions of the  
239 knee ligaments starting from a reproducible and repeatable landmark cloud virtually palpated  
240 on a CT scan. The proposed procedure has been evaluated through a comparison with the  
241 same estimations as obtained from MRI, which, as shown by Taylor et al. (2013) can be  
242 considered as a reliable reference.

243 Despite many studies have noted the importance of scaling anatomical landmarks from  
244 cadaveric specimen to calculate inaccessible points (Brand et al., 1982; Lew and Lewis,  
245 1977; Lewis et al., 1980), we are not aware of other studies providing a methodology to  
246 estimate the knee ligaments attachments from a CT scan. Other methods proposed to create  
247 subject-specific musculoskeletal models, focused on the mathematical development of the  
248 scaling technique needed to estimate the coordinates of bone points not accessible through  
249 manual palpation. The results reported show that our methodology allows calculating the  
250 knee ligaments attachments with an average RMS error of 2,4 mm on the femur and 2,9 mm  
251 on the tibia. The relevance of these errors certainly depends on the practical use of the  
252 estimated quantities. A sensitivity analysis of their effects on the estimation of additional  
253 parameters, such as ligaments strain during dynamic tasks, could be the objective of further  
254 studies.

255 True accuracy of our estimates should be assessed with *ex vivo* studies. The only study that  
256 we are aware of proposing a methodology to estimate inaccessible points that have been  
257 validated in-vitro is the one by Kepple et al. (1998), who reported RMS errors of 6.6 mm on  
258 the femur and 5,8 mm on the tibia. In a very recent study Pellikaan et al. (2014) reported a  
259 mesh morphing based method which allows to estimate the muscle attachment sites of the

260 lower extremity with a mean error smaller than 15 mm, as assessed through ex-vivo testing.  
261 This method is based on the assumptions that the bone geometry is strongly correlated with  
262 the muscle attachment sites. This assumption, as highlighted by the authors, was based on  
263 clinical experience and it may be not applied to pathological patients (D1) with bone  
264 deformities. It has to be pointed out, in addition, that these authors only analysed muscle  
265 insertions and data concerning the origins and insertions of the ligaments have not been  
266 reported.

267 The reproducibility analysis showed an absence of significant interactions both between and  
268 within factors, confirming that the virtual palpation procedure that provides the input of the  
269 method is not operator-dependent. In addition, one of the operators performed the virtual  
270 palpation within a different software environment and obtained results that were overlapping  
271 to those from the other operators in terms of repeatability. This suggests that the changeover  
272 of the virtual palpation software can occur without losing precision.

273 Repeatability findings suggest that an inevitable source of error for our method lies in the  
274 morphological differences between different subjects: some landmarks can be determined  
275 more precisely than others (see Table 1) since some anatomical regions of knee change  
276 substantially from subject to subject (Fehring et al., 2009). The variability we found, in  
277 addition, was likely also due to the fact that pathological knees, presenting irregular or  
278 deformed surfaces, were part of our dataset. Hence, it is conceivably to hypothesise that the  
279 expertise of the operators and the use of standard and well-defined guidelines for the  
280 definition of the anatomical landmarks for the virtual palpation can both contribute to  
281 improve the accuracy of the proposed procedure.

282 The RA created for the purpose of this study is calculated from three knee specimens  
283 obtained from donors of 70 years of age, and has been used to predict the ligament  
284 attachments for a population that was only slightly different in terms of age (65 years on

285 average). Future research should be conducted to verify whether the accuracy of the method  
286 could be compromised when used in subjects of a different age range.

287 In conclusion, keeping in mind the generalizability limitations imposed by the number of  
288 investigated knees, the proposed procedure can be deemed adequately robust. It allows  
289 estimating the origins and the insertions of the knee ligaments from a CT scan with an  
290 accuracy level that is equivalent to that reachable using MRI images. As such, this procedure  
291 can be used to improve the accuracy of dynamic patient specific knee models in order to have  
292 a better understanding of the forces and the strains on the knee structures, such as the  
293 ligaments, during static and locomotion activities.

294

## 295 **ACKNOWLEDGEMENT**

296 The authors would like to thank Medacta International SA (Castel San Pietro, CH) for  
297 providing one of the dataset and the technical support.

298

299

300

301

302

303

304

305

306

307 **REFERENCES**

- 308 Arnold, E.M., Ward, S.R., Lieber, R.L., Delp, S.L., 2010. A model of the lower limb for  
309 analysis of human movement. *Ann. Biomed. Eng.* 38, 269–279.
- 310 Bert, J.M., 1996. Custom total hip arthroplasty. *J. Arthroplasty* 11, 905–915.
- 311 Blankevoort, L., Huiskes, R., 1996. Validation of a three-dimensional model of the knee. *J.*  
312 *Biomech.* 29, 955–961.
- 313 Brand, R.A., Crowninshield, R.D., Wittstock, C.E., Pedersen, D.R., Clark, C.R., van Krieken,  
314 F.M., 1982. A model of lower extremity muscular anatomy. *J. Biomech. Eng.* 104, 304–  
315 310.
- 316 Ellingsen, L.M., Chintalapani, G., Taylor, R.H., Prince, J.L., 2010. Robust deformable image  
317 registration using prior shape information for atlas to patient registration. *Comput. Med.*  
318 *Imaging Graph.* 34, 79–90.
- 319 Fehring, T.K., Odum, S.M., Hughes, J., Springer, B.D., Beaver, W.B., 2009. Differences  
320 between the sexes in the anatomy of the anterior condyle of the knee. *J. Bone Joint Surg.*  
321 *Am.* 91, 2335–2341.
- 322 Grimpampi, E., Camomilla, V., Cereatti, A., De Leva, P., Cappozzo, A., 2014. Metrics for  
323 describing soft-tissue artefact and its effect on pose, size, and shape of marker clusters.  
324 *IEEE Trans. Biomed. Eng.* 61, 362–367.
- 325 Guess, T.M., Liu, H., Bhashyam, S., Thiagarajan, G., 2011. A multibody knee model with  
326 discrete cartilage prediction of tibio-femoral contact mechanics. *Comput. Methods*  
327 *Biomech. Biomed. Engin.*
- 328 Guess, T.M., Thiagarajan, G., Kia, M., Mishra, M., 2010. A subject specific multibody model  
329 of the knee with menisci. *Med. Eng. Phys.* 32, 505–515.
- 330 H. Bloemker, K., 2012. Computational Knee Ligament Modeling Using Experimentally  
331 Determined Zero-Load Lengths. *Open Biomed. Eng. J.*
- 332 Kepple, T.M., Sommer, H.J., Siegel, K.L., Stanhope, S.J., 1997. A three-dimensional  
333 musculoskeletal database for the lower extremities. *J. Biomech.* 31, 77–80.
- 334 Kia, M., Stylianou, A.P., Guess, T.M., 2014. Evaluation of a musculoskeletal model with  
335 prosthetic knee through six experimental gait trials. *Med. Eng. Phys.* 36, 335–44.
- 336 Lew, W.D., Lewis, J.L., 1977. An anthropometric scaling method with application to the  
337 knee joint. *J. Biomech.* 10, 171–181.
- 338 Lewis, J.L., Lew, W.D., Zimmerman, J.R., 1980. A nonhomogeneous anthropometric scaling  
339 method based on finite element principles. *J. Biomech.* 13, 815–824.

- 340 Morrison, J.B., 1970. The mechanics of the knee joint in relation to normal walking. J.  
341 Biomech. 3, 51–61.
- 342 Pellikaan, P., van der Krogt, M.M., Carbone, V., Fluit, R., Vigneron, L.M., Van Deun, J.,  
343 Verdonshot, N., Koopman, H.F.J.M., 2014. Evaluation of a morphing based method to  
344 estimate muscle attachment sites of the lower extremity. J. Biomech. 47, 1144–1150.
- 345 Radermacher, K., Portheine, F., Anton, M., Zimolong, A., Kaspers, G., Rau, G., Staudte,  
346 H.W., 1998. Computer assisted orthopaedic surgery with image based individual  
347 templates. Clin. Orthop. Relat. Res. 28–38.
- 348 Reggiani, B., Cristofolini, L., Varini, E., Viceconti, M., 2007. Predicting the subject-specific  
349 primary stability of cementless implants during pre-operative planning: Preliminary  
350 validation of subject-specific finite-element models. J. Biomech. 40, 2552–2558.
- 351 Shelburne, K.B., Pandy, M.G., 2002. A dynamic model of the knee and lower limb for  
352 simulating rising movements. Comput. Methods Biomech. Biomed. Engin. 5, 149–159.
- 353 Taylor, K.A., Cutcliffe, H.C., Queen, R.M., Utturkar, G.M., Spritzer, C.E., Garrett, W.E.,  
354 DeFrate, L.E., 2013. In vivo measurement of ACL length and relative strain during  
355 walking. J. Biomech. 46, 478–483.
- 356 Van Sint Jan, S., 2007. Color atlas of skeletal landmark definitions: guidelines for  
357 reproducible manual and virtual palpations. Elsevier Health Sciences.
- 358 Van Sint Jan, S., Della Croce, U., 2005. Identifying the location of human skeletal  
359 landmarks: why standardized definitions are necessary--a proposal. Clin. Biomech.  
360 (Bristol, Avon) 20, 659–60.
- 361 Woo, S.L.Y., Abramowitch, S.D., Kilger, R., Liang, R., 2006. Biomechanics of knee  
362 ligaments: Injury, healing, and repair. J. Biomech.
- 363 Zanetti, E.M., Crupi, V., Bignardi, C., Calderale, P.M., 2005. Radiograph-based femur  
364 morphing method. Med. Biol. Eng. Comput. 43, 181–188.
- 365 NMSBuilder (<http://www.nmsphysiome.eu/resources.html>), SCS srl, Italy

366

367

368

369

370

371 TABLES

372

Landmark	SD Min (mm)	SD Max(mm)
FLE	0.02	5.97
FBE	0.56	2.37
FUE	0.06	2.31
FME	0.38	5.30
FAM	0.16	3.02
FMC	0.08	3.04
FLC	0.04	1.74
FLG	0.16	2.67
FMG	0.06	3.18
FPS	0.23	7.71
FMS	0.31	6.46
TTC	0.1	7.67
TLR	0.03	4.72
TMR	0.11	3.99
TGT	0.22	3.91
LCL	0.03	1.38

373

**Table 1** – The table shows the precision of the landmark positions in terms of Standard Deviation.

374

	Mean Distance (mm)	Min (mm)	Max (mm)
SUBJECT 1	2,6 ± 0,8	1,8	4,2
SUBJECT 2	2,2 ± 0,9	1,1	4,5
SUBJECT 3	2,5 ± 1,8	0,3	5,8
SUBJECT 4	2,5 ± 1,6	0,2	5,1
SUBJECT 5	2,6 ± 2,3	0,7	7,3
SUBJECT 6	2,1 ± 0,8	0,7	3,3
SUBJECT 7	1,9 ± 1,1	0,6	4,2

375

**Table 2** – Registration Atlas registered on the seven subjects (femur)

376

	Mean Distance (mm)	Min (mm)	Max (mm)
SUBJECT 1	2,1 ± 1,1	0,6	2,9
SUBJECT 2	1,9 ± 1,9	0	3,7
SUBJECT 3	1,1 ± 0,4	0,7	1,6
SUBJECT 4	2,1 ± 1,2	0,5	3,1
SUBJECT 5	1,0 ± 0,6	0,3	1,7
SUBJECT 6	1,3 ± 0,8	0,4	2,2
SUBJECT 7	1,2 ± 0,7	0,4	2,2

377

**Table 3** – Registration Atlas registered on the seven subjects (tibia)

378  
379

	Mean Distance (mm)	Min (mm)	Max (mm)
SUBJECT 1	2,5 ± 2,9	0,0	5,5
SUBJECT 2	1,3 ± 2,3	0,1	4,7
SUBJECT 3	3,9 ± 2,8	0,0	6,3
SUBJECT 4	3,1 ± 3,9	0,0	8,0
SUBJECT 5	2,1 ± 1,9	0,0	4,7
SUBJECT 6	0,4 ± 0,7	0,0	1,4
SUBJECT 7	1,3 ± 2,6	0,0	5,3

380  
381  
382  
383

**Table 4** – Mean Distance between the insertion and the origin of the ligaments predicted and the ones estimated on the MRI images (femur)

	Mean Distance (mm)	Min (mm)	Max (mm)
SUBJECT 1	4,4 ± 4,2	0,0	10,2
SUBJECT 2	2,6 ± 1,8	0,0	4,1
SUBJECT 3	2,5 ± 5,1	0,0	10,2
SUBJECT 4	/	/	/
SUBJECT 5	1,4 ± 1,7	0,0	3,2
SUBJECT 6	2,8 ± 5,6	0,0	11,3
SUBJECT 7	2,7 ± 3,1	0,0	6,1

384  
385  
386  
387  
388  
389

**Table 5** – Mean Distance between the insertion and the origin of the ligaments predicted and the ones estimated on the MRI images (tibia). The subject 4 is not included in this comparison because the MRI data was incomplete

	Age at death	Gender	Right or Left	Height(in)	Weight(lbs)
Knee #1	77	Male	Right	70	220
Knee #2	55	Female	Left	67	160
Knee #3	78	Female	Right	65	130

390  
391  
392  
393  
394  
395  
396

**Table 6** – Information regarding each cadaver knee used in this study to create the Registration Atlas

397 **FIGURES**

398

399

400

401

402

403

404

405

406

407

408

409

410

411

412

413

414

415

416

417

418

419

420

421

422

423

424

425

426

427

428

429

430

431

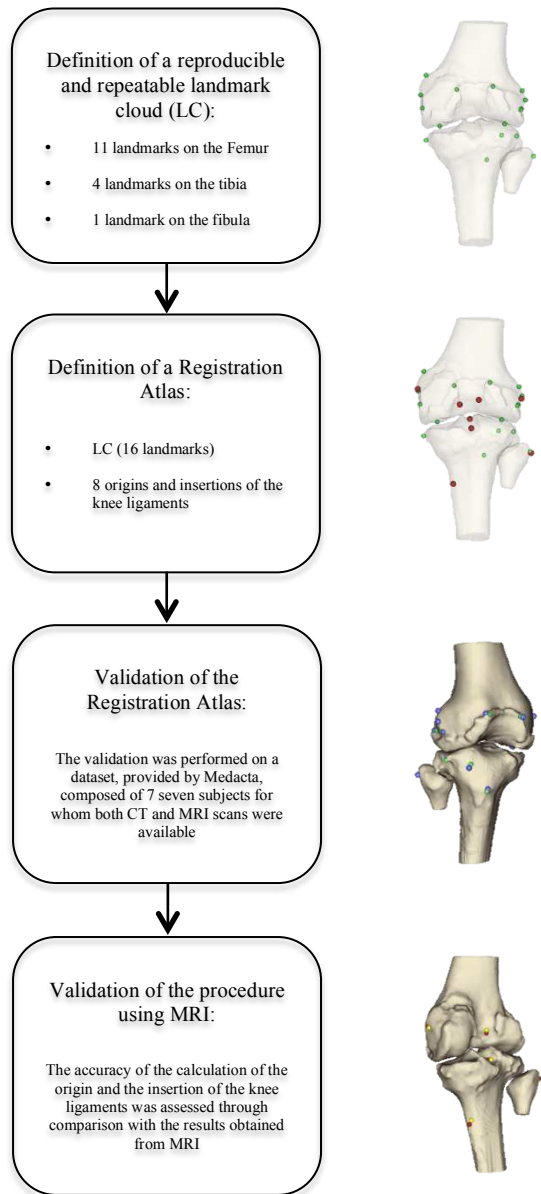
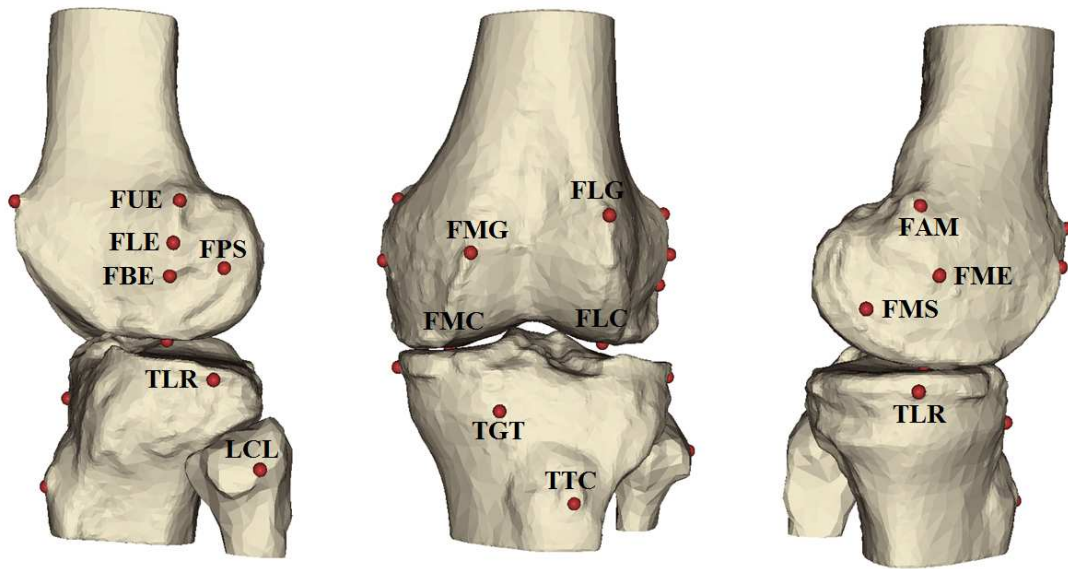


**Figure 1** - Schematic representation of the procedure: 1) Creation of a repeatable bone landmarks cloud palpable on CT scan images. 2) Definition of a reference landmarks cloud called Registration Atlas composed by reproducible and repeatable landmarks and the origin and insertion of the knee ligaments. 3) Validation of the RA 4) Calculation of the origin and insertion of the knee ligaments using CT scan and validation using MRI images

432

433



434

435

436

437

438

439

440

441

442

443

**Figure 2** – Set of landmarks selected using the “Colour Atlas of Skeletal Landmark Definitions” (Serge Van Sint Jan 2007). FME- Medial Epicondyle, FAM-Tubercle of the Adductor Magnus muscle, FMS-Medial Sulcus, FLE- Lateral Epicondyle, center of tubercle, FUE-Lateral Epicondyle, FBE Lateral Epicondyle, FPS-Popliteal Sulcus, FLG-Antero-Lateral ridge of the patellar surface Groove, FMG-Antero-Medial ridge of the patellar surface Groove, FLC-Most distal point of the Lateral Condyle, FMC-Most distal point of the Medial Condyle, TLR-Lateral Ridge of tibial plateau, TMR-Medial Ridge of tibial plateau, TGT -Gerdy Tubercle, TTM-Tibia, Tuberosity medial edge, LCL-Attachment of the collateral Lateral Ligament